Ex 1

DET NORSKE VIDENSKAPS-AKADEMI I OSLO

# GEOFYSISKE PUBLIKASJONER
## GEOPHYSICA NORVEGICA

VOL. XXVII. No. 2 January 1968

JÖRGEN HOLMBOE

# Instability of baroclinic three-layer models of the atmosphere



OSLO 1968
UNIVERSITETSFORLAGET

GEOFYSISKE PUBLIKASJONER

GEOPHYSICA NORVEGICA

VOL. XXVIII. NO. 2

# INSTABILITY OF BAROCLINIC THREE-LAYER MODELS OF THE ATMOSPHERE*

By Jørgen Holmboe

FREMLAGT I VIDENSKAPS-AKADEMIETS MØTE DEN 15. SEPTEMBER 1967

**Abstract.** The theory for unstable waves in a single baroclinic layer with a constant entropy gradient which was developed by Eady in 1949 [1] is generalized in this paper to bounded, vertically symmetric three-layer models with constant entropy gradients in each layer. With the use of the quasi-geostrophic approximation and the Bousinesq approximation, and with the planetary vorticity gradient of the earth ignored, the evolution of laterally unbounded symmetric waves in these models from arbitrary initial states, and the ultimate asymptotic approach of the long unstable waves to their stationary tilting state of the growing normal mode are described. It is shown that in all the models the longest waves have the same simple kinematic structure and the same limiting growth rate which are determined by the mean kinetic energy of the zonal thermal wind. The position of the spectral boundary between the shorter stable and the longer unstable waves and also the position and rate of growth of the fastest growing mode are moderately influenced by the vertical distribution of the entropy gradient. Models with parallel isentropes become more unstable when the buoyancy is concentrated near the center level, the maximum instability occurring when the entire entropy change is concentrated in a frontal discontinuity in the middle. Models with the same thermal wind in the layers become more stable when the buoyancy is concentrated near the center level. This apparent paradox is explained by simple energy considerations. The modifications of the instability of the model with the variations of the entropy gradient along the vertical are not very large except in extreme cases which do not resemble observed conditions in the atmosphere.

1. **The model.** The model is shown schematically in Fig. 1. It is bounded below by a rigid horizontal plane (the ground), and bounded above by another rigid horizontal plane (the tropopause) at the height 2h above the ground. The field of entropy is continuous and has a constant meridional gradient in the center layer, namely,

Center layer: $$\nabla \ln\theta = -\tau \boldsymbol{j} + \sigma \boldsymbol{k} \qquad (\tau \text{ and } \sigma \text{ positive and const.})$$

and a different constant gradient in the outer layers, namely

Outer layers: $$\nabla \ln\theta = -\tau_1 \boldsymbol{j} + \sigma_1 \boldsymbol{k} \qquad (\tau_1 \text{ and } \sigma_1 \text{ positive and const.})$$

* The research reported in this paper was sponsored by the National Science Foundation under grant G 22557.

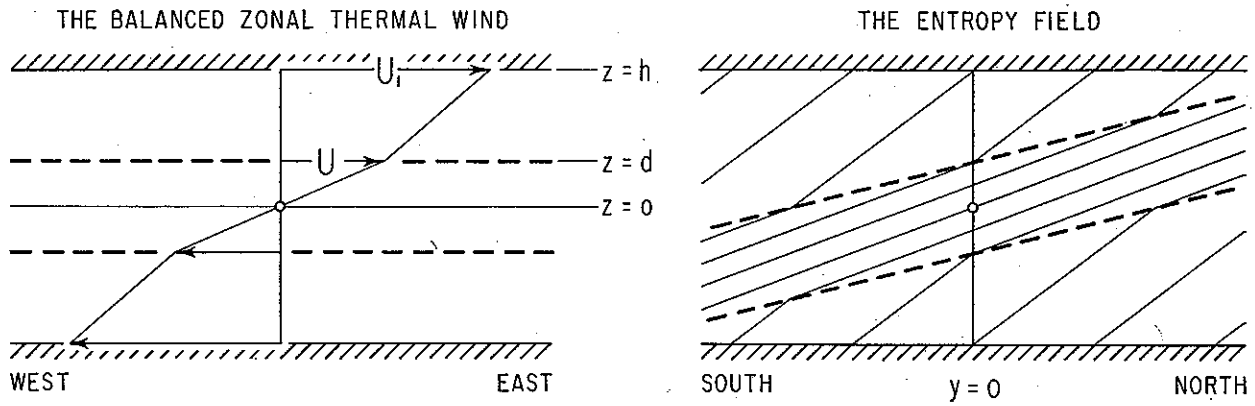


Fig. 1. Baroclinic three-layer model of the atmosphere.

The center layer has the constant depth 2d, and the meridional slope,

Center layer slope: $$\frac{dz}{dy}=\frac{\tau_1-\tau}{\sigma_1-\sigma}.$$

We shall consider conditions near a center latitude ($y=0$), where the center layer is in the middle, and we shall ignore the variation of the Coriolis parameter $f$ with latitude. The model is completely defined by the parameters of the center layer and the three non-dimensional ratios

(1.1) $$\delta=(h-d)/d, \qquad R=\tau_1/\tau, \qquad r=\sqrt{\sigma_1/\sigma}=N_1/N, \qquad (N=\sqrt{\sigma g})$$

where $N$ denotes the buoyancy frequency.

In the undisturbed state of the model the meridional entropy gradient is balanced by the proper zonal wind shear which, within the accuracy of the Bousinesq-approximation, has a constant value within each layer, namely

(1.2) $$fU_z=g\tau.$$

The zonal wind has no variation with latitude in the model. We shall use a frame of reference with the origin ($z=0$) at the center level and moving with the air at that level. In this 'symmetric' frame the model has dynamic and kinematic vertical symmetry with reference to the center level and latitude. The zonal wind speed at the boundaries of the center layer has here (from 1.2) the value

(1.3) $|z|=d$: $$U=g\tau d/f,$$

which we choose as the basic velocity parameter of the model. The zonal wind speed at the rigid boundaries of the outer layers is

(1.4) $|z|=h$: $$U_1=U(1+\delta R).$$

If we ignore the density variations within the model (consistent with the Bousinesq-approximation) the kinetic energy of the balanced zonal motion in the symmetric frame is

$$h\bar{U}^2 = d\int_0^d (zU/d)^2 dz + (h-d)\int_d^h [U + RU(z-d)/d]^2 dz,$$

which gives

$$\bar{U}^2 = \frac{1}{3}U^2(1+3\delta+3R\delta^2+R^2\delta^3)/(1+\delta). \tag{1.5}$$

The velocity $\bar{U}$ may be regarded as the zonal wind in an isentropic two-layer model which has the same kinetic energy as the baroclinic three-layer model.

**2. The quasi-geostrophic, adiabatic wave equations in a layer with constant entropy gradient.** We now superimpose on the balanced undisturbed model in section 1 a small-amplitude wave disturbance, which has a sinusoidal variation in the zonal direction and no variation in the meridional direction. Associated with the wave motion are sinusoidal deformations of the isentropic surfaces, so the entropy field in the center layer has the distribution

$$\ln\theta = \ln\theta_0 - \tau(y-Y) + \sigma z, \tag{2.1}$$

where $Y$ denotes the meridional departure of the isentropic surface from its equilibrium latitude. With $k = 2\pi/L$ denoting the wave number of the wave, the velocity and entropy deformation of the wave may be written

$$\begin{aligned} \boldsymbol{v} &= \text{Im. part of } V(z,t)\exp(ikx) \equiv u\boldsymbol{i} + v\boldsymbol{j} + w\boldsymbol{k}. \\ Y &= \text{Im. part of } A_c(z,t)\exp(ikx). \end{aligned} \tag{2.2}$$

During the evolution of the wave the physical changes of the air particles are adiabatic, so the isentropic surfaces are material surfaces containing the same air particles at all times. Thus, individual time differentiation in (2.1) gives the adiabatic equation

$$\sigma w = \tau(v - DY/Dt). \tag{2.3}$$

Next introduce the quasi-static and the quasi-geostrophic approximations in the equation of motion. The latter approximation implies instantaneous adjustment of the motion to geostrophic balance, and the accelerations during the adjustments ignored. Within the accuracy of the Bousinesq approximation, the vertical derivative of the quasi-static-geostrophic equation (using 2.1) is

$$f(U_z\boldsymbol{i} + v_z) = \boldsymbol{k}\times\nabla\ln\theta = g\tau(\boldsymbol{i} + Y_x\boldsymbol{j}).$$

The meridional component of this equation, using (1.2), gives the geostrophic thermal wind formula

$$Y_x = v_z/U_z, \tag{2.4}$$

which shows that the quasi-geostrophic wind shear is parallel to the isentropic contour lines.

The remaining dynamic principle which governs the motion is the conservation of potential vertical vorticity. The linearized vertical component of the vorticity equation has the complicated form

$$\frac{D}{Dt}(f+v_x) - fw_z - \tau\left[\frac{Du}{Dt} + (U_z+F)w - f(v-zv_z)\right] = 0 \tag{2.5}$$

where $F = 2\Omega \cos\phi$ is the horizontal Coriolis parameter. However, the kinematic terms in the brackets are multiplied by the meridional entropy gradient, and hence are ignored by the Boussinesq approximation. From the adiabatic equation (2.3) and use of the geostrophic equation (2.4) the convergence $w_z$ in (2.5) has the value

$$\sigma w_z = \tau(v - DY/Dt)_z = -\tau DY_z/Dt.$$

With this value substituted, the vorticity equation takes the form

$$\frac{D}{Dt}[f + v_x + f(\tau/\sigma)Y_z] = 0.$$

The quantity in the brackets is a geostrophic vorticity invariant.

With the latitude variation of the Coriolis parameter ignored, the zonal derivative of the geostrophic vorticity invariant, using (2.4 and 1.1,2), gives the differential equations for the meridional velocity in a meridionally unbounded disturbance of the three-layer model, namely

$$\begin{aligned} |z| < d: \quad & v_{xx} = -(f/N)^2 v_{zz}, \\ |z| > d: \quad & v_{xx} = -(f/rN)^2 v_{zz}. \end{aligned} \tag{2.6}$$

Since the model, to the accuracy of the Boussinesq- and ($\beta = 0$)-approximations, has dynamic and kinematic symmetry along the vertical with reference to the center level and latitude it is of interest to examine the behavior of symmetric waves in the model.

**3. The evolution of symmetric waves in quasi-geostrophic three-layer models.** We introduce for the wave in (2.2) the non-dimensional wave number

$$\kappa = kd(N/f), \tag{3.1}$$

and write the equations in (2.6) for the wave in (2.2) in terms of the correspondingly scaled height variables

$|z|<d$: $\quad v=(d/\kappa)^2 v_{zz}=v_{\xi\xi}; \qquad \xi=(\kappa/d)z$

$|z|>d$: $\quad v=(d/r\kappa)^2 v_{zz}=v_{\zeta\zeta}. \qquad \zeta=(r\kappa/d)(z-h).$

A symmetric wave which satisfies these equations has from an arbitrary initial state the evolution

$$\begin{aligned} z<d: &\quad v=\text{Im. part } [A(t)\cosh\xi+iB(t)\sinh\xi]e^{ikx}=V\sin(kx+\theta). \\ z>d: &\quad v=\text{Im. part } [A_1(t)\cosh\zeta+iB_1(t)\sinh\zeta]e^{ikx}=V\sin(kx+\theta). \end{aligned} \tag{3.2}$$

where the real time-dependent amplitudes $A$, $B$, etc. are determined by the boundary conditions. The condition of zero vertical motion at the rigid top of the upper layer (from 2.3,4) is represented by the equation

$z=h$: $\quad v=Y_t+U_1Y_x; \qquad RUY_x=dv_z=r\kappa v_\zeta,$

or with $Y$ eliminated

$z=h$: $\quad (R/r\kappa)Uv_x=(v_t+U_1v_x)_\zeta.$

With the upper boundary values of $v$ and its derivatives substituted from (3.2) and $U_1$ substituted from (1.4), the condition becomes

$$(R/r)A_1=\kappa[B_{1t}/(kU)+i(1+R\delta)B_1] \tag{3.4}$$

The condition of continuity of the motion across the upper boundary of the center layer is represented by the two equations

$z=d$: $\quad \Delta w=\Delta[\tau/\sigma(v-Y_t-UY_x]=0; \qquad \Delta v=0,$

where $\Delta$ denotes the difference between the values above and below the boundary. With $Y$ eliminated, using (2.4), the $\Delta w$-equation takes the form

$$z=d: \quad (r-R/r)Uv_x=\kappa r(v_t+Uv_x)_\xi-\kappa(v_t+Uv_x)_\zeta; \qquad \Delta v=0. \tag{3.5}$$

With the boundary values of $v$ and its derivatives substituted from (3.2) these are two homogeneous equations in the amplitudes $A$, $B$, $A_1$ and $B_1$ and their time derivatives. From these $A_1$ and $B_1$ may be expressed in terms of $A$ and $B$, and substituted in (3.4). The real and imaginary parts of the resulting equation are the evolution equations for the amplitude and phase of the center layer meridional velocity (the vorticity field) of the symmetric wave in (3.2). They may be written non-dimensionally in fairly compact forms, namely

$$\begin{aligned} p(\kappa A_t-b'B)_t&=q\tanh\kappa(\kappa B_t+aA), \\ p(\kappa A_t-bB)&=-q\tanh\kappa(\kappa B_t+a'A)_t, \end{aligned} \qquad (kU=1) \tag{3.6}$$

where we have introduced the abbreviations

$$
\begin{aligned}
&p = r^{-1}\tanh\alpha + \tanh\kappa, \quad && P = 1 + r\tanh\alpha\tanh\kappa, && \alpha = \delta r\kappa = -\zeta(z=d),\\
&q = r^{-1}\tanh\alpha + \coth\kappa, && Q = 1 + r\tanh\alpha\coth\kappa, && K = \kappa(1+\delta R),\\
&a' = \frac{Kp - \rho P + (\rho-1)}{q\tanh\kappa}, && a = \frac{Kp - \rho P + (\rho-1)\gamma/\kappa}{q\tanh\kappa}, && \rho = R/r^2,\\
&b' = \frac{Kq - \rho Q + (\rho-1)}{p\coth\kappa}, && b = \frac{Kq - \rho Q + (\rho-1)\gamma/\kappa}{p\coth\kappa}, && \gamma = K - \rho r\tanh\alpha.
\end{aligned}
\tag{3.7}
$$

These evolution equations in (3.6) are greatly simplified when applied to models where the isentropic surfaces are parallel in the three layers. In these models $R=r^2$ or $\rho=1$, so, from (3.7)

$$
R=r^2: \quad a=a'=\coth\kappa(Kp-P)/q\,; \qquad b=b'=\tanh\kappa(Kq-Q)/p, \tag{3.8}
$$

and the product of the two equations in (3.6) gives

$$
p^2(\kappa A_t - bB)_t^2 + q^2\tanh^2\kappa(\kappa B_t + aA)_t^2 = 0,
$$

which is satisfied by the simple linear evolution equations

$$
A_t/B = b/\kappa\,; \qquad B_t/A = -a/\kappa. \tag{3.9}
$$

The symmetric waves which have this evolution in models with parallel isentropes are examined in the next section.

**4. The evolution of symmetric waves in three-layer models with parallel isentropes.** The evolution equations in (3.9) for waves in these models are easily derived directly from the boundary conditions in (3.4) and (3.5). The conditions in (3.5) are here greatly simplified, because the boundaries of the center layer are isentropic surfaces, so the thermal wind is continuous across these boundaries. The conditions in (3.5) are therefore here

$$
z=d: \qquad rv_\xi = v_\zeta\,; \qquad \Delta v = 0,
$$

or with the values of $v$ substituted from (3.2)

$$
\begin{aligned}
A_1 &= A(\cosh\alpha\cosh\kappa + r\sinh\alpha\sinh\kappa) + iB(\cosh\alpha\sinh\kappa + r\sinh\alpha\cosh\kappa),\\
iB_1 &= A(\sinh\alpha\cosh\kappa + r\cosh\alpha\sinh\kappa) + iB(\sinh\alpha\sinh\kappa + r\cosh\alpha\cosh\kappa).
\end{aligned}
\tag{4.1}
$$

With these values substituted in (3.4), the real and imaginary parts of the resulting equation, with the abbreviations in (3.7) and (3.8), are in fact the two evolution equations in (3.9).

With the amplitudes $A$ and $B$ of the sine and cosine waves replaced by the amplitude and phase of the resultant wave, as indicated in (3.2),

$$A\cosh\xi = V\cos\theta, \qquad B\sinh\xi = V\sin\theta, \tag{4.2}$$

and the dimensions restored, the evolution equations in (3.9) become

$$\frac{(V\sin\theta)_t}{V\cos\theta} = -\left(\frac{Uk}{\kappa}\right)a\tanh\xi = (\ln V)_t\tan\theta + \theta_t = c_a(\theta=0),$$
$$\frac{(V\cos\theta)_t}{V\sin\theta} = \left(\frac{Uk}{\kappa}\right)b\coth\xi = (\ln V)_t\cot\theta - \theta_t = -c_b(\theta=90^0). \tag{4.3}$$

These give the evolution in the center layer of the symmetric wave from an arbitrary initial state. In the non-tilting states, $\theta=0$ and 90°, the wave is instantaneously neutral, and it moves through these states with the phase speeds $c_a$ and $c_b$ indicated in (4.3). In terms of these, the growth rate and phase velocity of the wave in an arbitrary state are

$$\theta_t = c_a\cos^2\theta + c_b\sin^2\theta.$$
$$(\ln V)_t = \tfrac{1}{2}(c_a - c_b)\sin 2\theta. \tag{4.4}$$

The time derivative of the phase velocity equation is

$$(\ln\theta_t)_t = -(c_a - c_b)\sin 2\theta,$$

which, combined with the growth rate equation, gives

$$(\theta_t V^2)_t = 0. \tag{4.5}$$

Thus, at every level the wave energy transport relative to the symmetric frame remains constant during the evolution of the wave.

The evolution is determined by the parameters $a$ and $b$ in (3.8). The parameter $b$ is positive for all wave lengths, so all waves move downwind through the non-tilting *b-state* ($\theta=90°$). The parameter $a$, on the other hand, is positive for short waves and negative for long waves, and is zero for the ($Kp=P$)-wave. This wave has a stationary neutral *a-state* ($\theta=0$) with a non-tilting wave trough. It represents the spectral boundary between the shorter stable waves, which move progressively downwind at all times, and the longer unstable waves which move upwind through the a-state.

The wave number $\kappa_s$ of this stability boundary wave is, from (3.7,8), determined by the transcendental equation

$$a=0: \qquad \kappa_s(1+\delta r^2)(\tanh\kappa_s + r^{-1}\tanh\alpha) = 1 + r\tanh\alpha\tanh\kappa_s \qquad (\alpha=\delta r\kappa_s). \tag{4.6}$$

The wave number $\kappa_0$ of the gravity wave with the frequency $f$ in the same model (see Appendix A) is given by

$$\tan\kappa_0 = r\cot\alpha_0 \qquad (\alpha_0=\delta r\kappa_0). \tag{A.2}$$

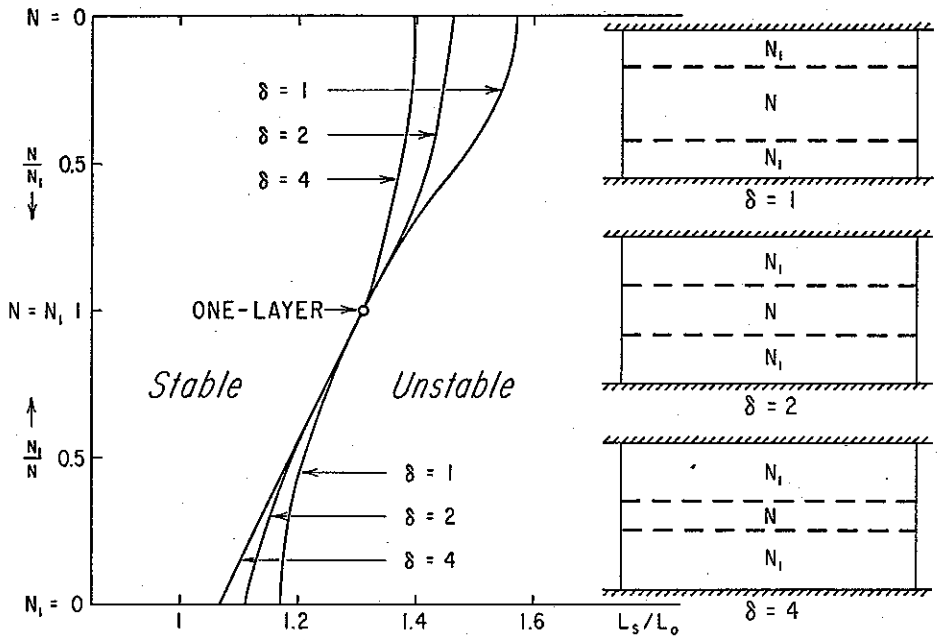


Fig. 2. Stability boundary in three-layer models with parallel isentropes. *Lé* is length of gravity wave with frequency $f$.

The ratio of these gives the wave length $L_s$ of the stability boundary wave in units of the wave length of the gravity wave with the frequency $f$ in the model. It is shown by the three lines in Fig. 2 as function of the buoyancy ratio $r=N_1/N$ for three different models with the depth ratios $\delta=(h-d)/d=1,2,4$.

For the limiting models with isentropic center layer ($N=0$) and with isentropic outer layers ($N_1=0$) the stability boundary equations are

(4.7)

$$N_1=0: \qquad \kappa_s \tanh\kappa_s+\delta\kappa_s^2=1\,, \qquad \kappa_0=\cot\kappa_0/\delta\,.$$

$$N=0: \qquad \hat{\kappa}_s \tanh\hat{\kappa}_s(\delta-1)=1-\delta\hat{\kappa}_s^2\,, \qquad \hat{\kappa}_0=\tfrac{1}{2}\pi/\delta\,.$$

where

$$\hat{\kappa}=r\kappa=kd(N_1/f)\,.$$

When the three layers have the same buoyancy ($N=N_1$) the model is the one-layer model with a constant entropy gradient between the outer rigid boundaries which was investigated by EADY. Here the stability boundary equation reduces to EADY's equation [1]

(4.8) $N=N_1$:

$$K_s \tanh K_s=1\,, \qquad K_s=\kappa_s(1+\delta)=k_s h(N/f)=1.1997\,.$$

$$\tan\kappa_0=\cot\delta\kappa_0\,; \qquad K_0=\kappa_0(1+\delta)=k_0 h(N/f)=\tfrac{1}{2}\pi\,.$$

The stability boundary in Eady's model is at $L_s=1.31\,L_0$.

The general rule which is illustrated in Fig. 2 is that the stability boundary moves toward shorter waves and the model becomes more unstable as the buoyancy is concentrated in the center layer, while the overall static stability, as measured by the speed of the gravity waves, remains constant.

**5. The evolution of the short stable ($\varkappa > \varkappa_s$)-waves.** Here the phase velocities $c_a$ and $c_b$ in the non-tilting states of the wave have the same sign (see 4.3) so, from (4.4), the waves shorter than the stability boundary wave move progressively downwind at all times. Their evolution is governed by the unchanging energy transport in (4.5), namely

$$\theta_t V^2 = c_a V_a^2 = c_b V_b^2 = V_a V_b \sqrt{c_a c_b},$$

or with $\theta_t$ substituted from (4.4)

$$\left(\frac{V\cos\theta}{V_a}\right)^2 + \left(\frac{V\sin\theta}{V_b}\right)^2 = 1. \qquad (a>0) \tag{5.1}$$

The evolution of amplitude and phase of the short stable waves is represented in a polar amplitude-phase plane by an ellipse, which is traced with constant areal velocity with the period $T = 2\pi/\sqrt{c_a c_b}$ or, from (4.3), with the wave frequency

$$m = 2\pi/T = \sqrt{c_a c_b} = \sqrt{ab}(Uk/\kappa). \qquad (a>0) \tag{5.2}$$

For the very short waves the parameters $a$ and $b$ in (3.8) have the same limiting positive value, namely

$$\kappa \to \infty: \qquad p \to q \to 1 + r^{-1}; \qquad P \to Q \to 1 + r; \qquad a \to b \to K = \kappa(U_1/U).$$

The shortest waves are neutral waves which move downwind in the symmetric frame with the frequency $m = kU_1$.

**6. The evolution of the long unstable ($\varkappa < \varkappa_s$)-waves.** These waves move downwind through the $b$-state ($\theta = 90°$) and upwind through the $a$-state ($\theta = 0$). In either case the evolution is governed by the constant energy transport,

$$\theta_t V^2 = c_a V_a^2 \text{ or } c_b V_b^2.$$

From an arbitrary initial state the wave approaches asymptotically a stationary tilting state with the phase $\theta_s$, which, from (4.4), is given by

$$\tan^2\theta_s = -c_a/c_b = (-a/b)\tanh^2\xi. \qquad (\theta_t = 0) \tag{6.1}$$

The evolution from the $a$-state toward this state is represented in the amplitude-phase plane by the hyperbola

$$\left(\frac{V\cos\theta}{V_a}\right)^2 - \left(\frac{V\sin\theta}{V_a\tan\theta_s}\right)^2 = 1, \qquad (a<0) \tag{6.2}$$

which is traced with the constant areal velocity $\frac{1}{2}c_a V_a^2$ as the wave moves upwind from the $a$-state. As the wave approaches the stationary state with the asymptotic phase $\theta_s$, the wave ultimately, as $\theta_t \to 0$, grows at the constant exponential rate in (4.3), namely

$$(\ln V)_t = n = \sqrt{-c_a c_b} = \sqrt{-ab}(Uk/\kappa). \qquad (a<0). \tag{6.3}$$

The stationary growing state of the wave in (6.1,3) is the growing normal mode of the three-layer model. The model has also a decaying normal mode which has the stationary downwind tilting phase $\theta_s$ in (6.1) and decays exponentially at the rate $n$ in (6.3). If the wave has an initial state very near and upwind from the state of the decaying mode, its evolution is represented by the amplitude-phase hyperbola through the $a$-state. As the wave moves upwind from this state the hyperbola is traced with constant areal velocity, and the wave decays to the minimum amplitude and maximum speed in the $a$-state, and from there continues upwind with growing amplitude and diminishing speed toward the asymptotic state of the growing mode.

For the very long waves the values of the parameters $p,P$ and $q,Q$ in (3.7) with $R=r^2$ to the order of $\kappa^2$ are

$$p=\kappa(1+\delta); \qquad \kappa q = 1+\frac{1}{3}\kappa^2(1+3\delta);$$

$\kappa \to 0$:

$$P=1+R\delta\kappa^2; \qquad Q = 1+R\delta+\frac{1}{3}\kappa^2(R\delta-R^2\delta^3);$$

and the values of the parameters $a$ and $b$ to the same order are

$$a=-1+\kappa^2(1+2\delta+R\delta^2)$$

$\kappa \to 0$:

$$b=\frac{1}{3}\kappa^2(1+3\delta+3R\delta^2+R^2\delta^3)/(1+\delta)=(\kappa\bar{U}/U)^2$$

where $\bar{U}^2$ is the mean kinetic energy of the undisturbed balanced zonal motion in the symmetric frame (see 1.5). With these substituted in (6.3) we see that the growth rate of the very long waves has the value $n=k\bar{U}$. It is governed only by the mean kinetic energy of the baroclinic zonal wind shear and the wave length. It is not affected by the buoyancies and the depths of the layers. We shall show in Appendix B that the very long waves have the growth rate $k\bar{U}$ in any baroclinic layer with arbitrary distribution of wind shear and buoyancy between the rigid boundaries.

The growth rate of the normal mode in (6.3), measured in units of the inertial frequency $f=k_0 C_L$ (see Appendix A) is

$$n/f = \sqrt{-ab}(U/\bar{U}\kappa_0)(\bar{U}/C_L). \tag{6.4}$$

The ratio $\bar{U}/U$ in (1.5) and the non-dimensional wave number $\kappa_0$ of the gravity wave with the frequency $f$ (see A.2) are functions of the model parameters $R$, $r$, $\delta$ in (1.1) and hence are characteristic constants for each model. The parameters $a$ and $b$ in

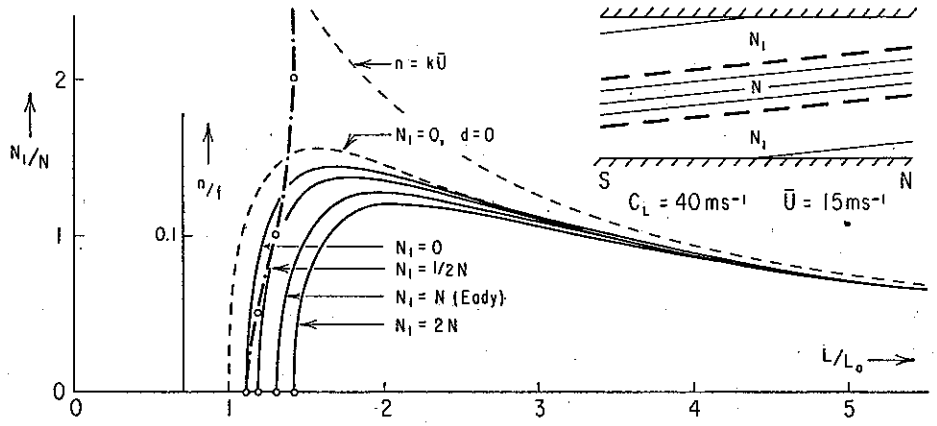


Fig. 3. Stability boundary and growth rate in models with parallel isentropes and equal depths of the layers. $L_0$ is length of gravity wave with frequency $f$.

(3.8) are also functions of the model parameters and the non-dimensional wave number $\kappa$. If further the mean kinetic energy and the overall static stability are specified, the growth rate $n/f$ is obtained from (6.4) for each wave length $L/L_0=\kappa_0/\kappa$. The values are shown in Fig. 3 for four models. All four have equal depths of the three layers ($\delta=2$), and the same kinetic energy and static stability given by $\bar{U}=15ms^{-1}$ and $C_L=40ms^{-1}$. The models are:

(i) *Eady's one layer model* ($N=N_1$). Here the parameters $a$ and $b$ in (3.8) reduce to Eady's values

$$N=N_1: \qquad \begin{matrix} P=q\tanh\kappa=1+\tanh\kappa\tanh\delta\kappa, & a=K\tanh K-1, \\ Q=p\coth\kappa=1+\coth\kappa\tanh\delta\kappa, & b=K\coth K-1, \end{matrix} \qquad K=\kappa(1+\delta)=kh(N/f).$$

And the wave number of the gravity wave with the frequency $f$, as in (4.8), is given by

$$r=1: \qquad \tan\kappa_0=\cot\delta\kappa_0: \qquad K_0=\kappa_0(1+\delta)=k_0h(N/f)=\tfrac{1}{2}\pi.$$

The stability boundary in the Eady model (see 4.8) is at $L_s=1.31L_0$. The wave number of the fastest growing wave is given by

$$\frac{d}{dK}(ab)=0: \qquad K_m=\frac{\sinh 4K_m}{3+\cosh 4K_m}=0.803; \qquad L_m/L_0=1.95.$$

The parameters $a$ and $b$ have here the values, $a=-0.465$, $b=0.206$, so from (6.3,4) the maximum growth rate is

$$n_m=0.310(U_1k/K_m); \qquad n_m/f=0.341(\bar{U}/C_L).$$

(ii) *Model with isentropic outer layers* ($r=0$). Here the parameters in (3.7) have the values

$$K=\kappa, \qquad \alpha/r=\delta\kappa, \qquad P=Q=1$$

$N_1=0$:

$$p=\delta\kappa+\tanh\kappa\,; \qquad q=\delta\kappa+\coth\kappa$$

and the parameters $a$ and $b$ in (3.8) are

$$N_1=0: \qquad a=\frac{\kappa\tanh\kappa+\delta\kappa^2-1}{1+\delta\kappa\tanh\kappa}\,; \qquad b=\frac{\kappa\coth\kappa+\delta\kappa^2-1}{1+\delta\kappa\coth\kappa}.$$

They reduce to Eady's one-layer values as the depths of the outer layers go to zero.

The model with the depth ratio $\delta=2$, whose growth rates are shown in Fig. 3, has the stability boundary at

$$N_1=0,\ \delta=2,\ a=0: \qquad \kappa_s=(1-\delta\kappa_s^2)\coth\kappa_s=0.5877.$$

The wave number of the gravity wave with the frequency $f$ in this model is

$$N_1=0,\ \delta=2: \qquad \kappa_0=\delta^{-1}\cot\kappa_0=0.6533.$$

The ratio of these give the wave length of the stability boundary at $L_s=1.11L_0$.

The energy ratio in (1.5) is

$$R=0,\ \delta=2 \qquad (\bar{U}/U)^2=7/9, \text{ which gives: } \kappa_0\bar{U}/U=0.576.$$

In this model both the stability boundary and the fastest growing wave have shorter wave lengths than in Eady's equivalent two-layer model, and the unstable waves have a faster growth. It appears that the instability is augmented by concentrating the static stability buoyancy toward the center of the model.

The maximum instability comes when the depth of the center layer shrinks to zero. With $\theta_t$ and $\theta_b$ denoting the potential temperatures of the remaining outer isentropic layers, we have then

$$d\to 0: \qquad \sigma d\to(\theta_t-\theta_b)/(\theta_t+\theta_b), \qquad \kappa\to 0, \qquad \delta\kappa^2=(k/k_0)^2=\lambda^{-1}.$$

The corresponding limiting values of the parameters $a$ and $b$ in this isentropic two-layer model are

$$d\to 0: \qquad a\to(1-\lambda)/(1+\lambda)\,; \qquad b\to\kappa^2\to 0.$$

When substituted in (6.3,4) these give the well known growth rate for the waves in the isentropic two-layer model, namely

$$d\to 0: \qquad n\to\sqrt{\frac{\lambda-1}{\lambda+1}}\cdot Uk\,; \qquad \frac{n}{f}=\sqrt{\frac{\lambda-1}{\lambda(\lambda+1)}}\cdot\frac{\bar{U}}{C_L}$$

see HOLMBOE [5].

This growth rate is shown in Fig. 3 as a thin broken line above the four other $n$-lines. The stability boundary is at $L_s=L_0$, and the fastest growing wave at

$L_m=(\sqrt{2}+1)^{\frac{1}{2}}L_0=1.55L_0$ has the growth rate

$$n_m/f=(\sqrt{2}-1)\bar{U}/C_L=0.414\bar{U}/C_L.$$

It represents the limiting growth rate in a baroclinic model with given static stability and kinetic energy.

(iii) *Model with weak buoyancy in outer layers* ($r=\frac{1}{2}$). Here the parameters in (3.7) have the values

$$\alpha=\kappa, \qquad K=3\kappa/2, \qquad p=3\tanh\kappa, \qquad q=\coth\kappa+2\tanh\kappa$$

$N_1=\frac{1}{2}N$, $\delta=2$:

$$P=1+\tfrac{1}{2}\tanh^2\kappa, \qquad Q=3/2.$$

and the $(a, b)$-parameters in (3.8) are

$$N_1=\tfrac{1}{2}N,\ \delta=2: \qquad a=\frac{\frac{1}{2}\tanh\kappa(9\kappa-\tanh\kappa)-1}{1+2\tanh^2\kappa}; \qquad b=\kappa(\tanh\kappa+\tfrac{1}{2}\coth\kappa)-\tfrac{1}{2}.$$

The wave number of the gravity wave with the frequency $f$ is

$$N_1=\tfrac{1}{2}N,\ \delta=2: \qquad \tan^2\kappa_0=\tfrac{1}{2}, \qquad \kappa_0=0.6155.$$

The energy ratio in (1.5) is

$$R=\tfrac{1}{4},\ \delta=2: \qquad (\bar{U}/U)^2=7/6, \quad \text{which gives } \kappa_0\bar{U}/U=0.664.$$

The stability boundary is here given by

$$N_1=\tfrac{1}{2}N,\ \delta=2,\ a=0: \qquad \kappa_s=(2\coth\kappa_s+\tanh\kappa_s)/9=0.5190,$$

so it has the wave length $L_s=1.186L_0$. As should be expected, the waves in this model have growth rates between the values in Eady's one-layer model and the isentropic outer layer model.

(iv) *Model with strong buoyancy in outer layers* ($r=2$). Here the parameters in (3.7) have the values

$$r=2: \qquad \alpha=4\kappa, \qquad p=\tanh\kappa+\tfrac{1}{2}\tanh 4\kappa, \qquad P=1+2\tanh\kappa\tanh 4\kappa$$

$$\delta=2: \qquad K=9\kappa, \qquad q=\coth\kappa+\tfrac{1}{2}\tanh 4\kappa, \qquad Q=1+2\coth\kappa\tanh 4\kappa.$$

The stability boundary is given by

$$Kp=P: \qquad \kappa_s=(1+2\tanh\kappa_s\tanh 4\kappa_s)/9(\tanh\kappa_s+\tfrac{1}{2}\tanh 4\kappa_s)=0.2453.$$

The wave number of the gravity wave with the frequency $f$ is given by

$$\tan\kappa_0\tan 4\kappa_0=2, \qquad \kappa_0=0.3478.$$

The stability boundary wave has the wave length $L_s=1.42L_0$.

The energy ratio in (1.5) is

$$R=4,\ \delta=2: \qquad (\bar{U}/U)^2=20.3, \quad \text{which gives } \kappa_0\bar{U}/U=1.567$$

The growth rates of the unstable modes in this model, shown by the lowest $n$-line in Fig. 3, are smaller than in Eady's model with uniform buoyancy. The instability of the model is weakened by concentrating the buoyancy toward the boundaries of the model.

**7. The kinematic structure of the growing modes in three-layer models with parallel isentropes.** In an arbitrary state the symmetric wave has the center layer meridional velocity field in (3.2), namely

$$|z|<d: \qquad v=A\cosh\xi\sin kx+B\sinh\xi\cos kx=V\sin(kx+\theta).$$

Associated with this field is a geostrophically balanced deformation of the entropy field, so the isentropic contour lines have the meridional slope in (2.4), namely

$$|z|<d: \qquad (U/\kappa)Y_x=v_\xi=A\sinh\xi\sin kx+B\cosh\xi\cos kx=(U/\kappa)A_c k\cos(kx-\sigma).$$

The amplitude $A(t)$ is the meridional velocity amplitude at the center level. Let us relabel this amplitude, and the amplitude ratio of the cosine and the sine wave as follows

$$(7.1) \qquad A(t)\equiv V_0(t); \qquad B(t)/A(t)\equiv R(t).$$

With these notations the meridional velocity field and the entropy field of the symmetric wave in the center layer are

$$|z|<d: \qquad v=V_0(t)\sec\theta\cosh\xi\sin(kx+\theta), \qquad \tan\theta=\tanh\xi\cdot R(t)$$

$$(Uk/\kappa)Y=V_0(t)\operatorname{cosec}\sigma\sinh\xi\sin(kx-\sigma), \qquad \tan\sigma=\tanh\xi/R(t).$$

With $A_s$ denoting the streamline amplitude of the resultant field, the ratio of the contour amplitude to the streamline amplitude in the center layer is

$$(7.2) \quad |z|<d: \qquad A_c/A_s=(\xi\tanh\xi)\cos\theta/\sin\sigma$$

An arbitrary initial state of the symmetric wave is defined by initial values of the center level amplitude $V_0$ and the amplitude ratio $R$. These in turn give the initial phase, $\tan\theta=R\tanh\xi$, and the initial amplitude $V=V_0\sec\theta\cosh\xi$, at every level of the center layer. The evolution of the wave from this state, as we have seen, is represented in the amplitude-phase plane by an ellipse for the short stable waves, by a hyperbola for the long unstable waves, which are traced with a constant areal velocity from the initial state.

The unstable waves, from any initial state, approach the stationary state of the growing mode with the growth rate $n$ in (6.4) and the wave elements

$$(7.3) \quad |z|<d: \qquad v=V_0e^{nt}\cosh\xi\sec\theta_s\sin(kx+\theta_s), \qquad \tan\theta_s=\sqrt{-a/b}\ \tanh\xi. \qquad (a<0)$$

$$(Uk/\kappa)Y=V_0e^{nt}\sinh\xi\operatorname{cosec}\sigma_s\sin(kx-\sigma_s), \qquad \tan\sigma_s=\sqrt{-b/a}\ \tanh\xi.$$

The vorticity wave tilts upwind, and the temperature wave tilts downwind. The tilt of the temperature wave comes from the growing inflation of the entropy lamellas in the region of convergence. The contour amplitude has the simple height variation

$|z|<d$: $$A_c=A_{c0}\sqrt{1+\left(1-\frac{b}{a}\right)\sinh^2\xi}\,. \qquad (a<0)$$

The upper layer field is obtained from (3.2) with the values of $A_1$ and $B_1$ substituted from (4.1). With the origin of the height variable $\zeta$ shifted from the top to the base of the upper layer:

(7.4) $$\eta=\zeta+\alpha=\frac{r\kappa}{d}(z-d), \qquad \text{(see 3.7)}$$

the meridional velocity field in the upper layer becomes

$z>d$: (7.5)
$$v=A(\cosh\kappa\cosh\eta+r\sinh\kappa\sinh\eta)\sin kx+$$
$$+B(\sinh\kappa\cosh\eta+r\cosh\kappa\sinh\eta)\cos kx=V\sin(kx+\theta).$$

The isentropic contours of the geostrophically balanced temperature field have (from 2.4) the meridional slope

$z>d$:
$$(rU/\kappa)Y_x=v_\eta=A(\cosh\kappa\sinh\eta+r\sinh\kappa\cosh\eta)\sin kx+$$
$$+B(\sinh\kappa\sinh\eta+r\cosh\kappa\cosh\eta)\cos kx=(rU/\kappa)A_c k\cos(kx-\sigma).$$

With the amplitudes $A$ and $B$ replaced by the center level amplitude and the amplitude ratio in (7.1), these upper layer fields of the symmetric wave become

(7.6) $z>d$:
$$v=V_0(t)\sec\theta(\cosh\kappa\cosh\eta+r\sinh\kappa\sinh\eta)\sin(kx+\theta),$$
$$(rkU/\kappa)Y=V_0(t)\operatorname{cosec}\sigma(\cosh\kappa\sinh\eta+r\sinh\kappa\cosh\eta)\sin(kx-\sigma),$$

where the phase angles have the values

(7.7) $z>d$: $$\tan\theta=\frac{\tanh\kappa+r\tanh\eta}{1+r\tanh\kappa\tanh\eta}\cdot R(t)\,; \qquad \tan\sigma=\frac{r\tanh\kappa+\tanh\eta}{r+\tanh\kappa\tanh\eta}/R(t).$$

The lower layer fields are symmetric images of these upper layer fields. With $r=1$ and $\kappa+\eta=\xi$, the model is Eady's one layer model, and the outer fields are uniform continuations of the center fields.

The ratio of the contour amplitude to the streamline amplitude in the symmetric frame in the upper layer is

$z>d$: $$A_c/A_s=(\kappa+r\eta)\frac{r^{-1}\tanh\eta+\tanh\kappa}{1+r\tanh\eta\tanh\kappa}\cdot\frac{\cos\theta}{\sin\sigma}$$

The asymptotic stationary fields of the unstable modes in the upper layer are obtained from (7.6,7) by substituting

$$V_0(t)\to V_0e^{nt}, \qquad R(t)\to\sqrt{-a/b} \qquad (a<0).$$

At the rigid top of the upper layer where $\eta=\alpha$, the phase angles in (7.7) for the growing mode are given by

$$z=h: \qquad \tan\theta_s=\tanh\kappa\cdot\frac{Q}{P}\cdot\sqrt{-\frac{a}{b}} \quad ; \qquad \cot\sigma_s=\tanh\kappa\cdot\frac{q}{p}\cdot\sqrt{-\frac{a}{b}} \quad ,$$

and the contour-streamline amplitude ratio is

$$z=h: \qquad A_c/A_s=(Kp/P)(\cos\theta_s/\sin\sigma_s)\equiv\sin(\theta_s+\sigma_s)\,,$$

so the horizontal streamlines at the rigid boundaries are parallel to the contours at the contour nodes.

**8. Relation between the divergence field and the vorticity field in meridionally unbounded waves.** When the wave has no variation with latitude the horizontal divergence is given by $u_x=-w_z$, and the vertical vorticity equation (2.5) in a local frame, which moves intrinsically with the air at the level we consider, has the form,

$$v_{xt}=-fu_x\,.$$

Let the wave trough be located in the region of convergence with the phase $\phi$ *upwind* from the divergence node,

$$(8.1) \qquad v=V\sin(kx+\phi)\,; \qquad u=-D\cos kx\,.$$

With these substituted, the vorticity equation becomes

$$(V\cos\phi)_t\sin kx+(V\sin\phi)_t\cos kx=fD\cos kx\,,$$

which gives

$$(8.2) \qquad (\ln V)_t=f(D/V)\sin\phi=\phi_t\tan\phi\,.$$

$$\phi_t=f(D/V)\cos\phi\,.$$

Here $\phi_t$ is the intrinsic upwind phase speed of the vorticity wave through the air. It is the sum of the upwind speed $\theta_t$ in the symmetric frame and the speed of the air in this frame, namely

$$(8.3) \qquad z<d: \qquad \phi_t=\theta_t+Uk(\xi/\kappa)\,,$$

$$z>d: \qquad \phi_t=\theta_t+Uk(1+r\eta/\kappa)\,.$$

The equations (8.2) show explicitly that the growth of the vorticity amplitude is governed by the convergence in the wave trough, and its intrinsic propagation through the air is governed by the convergence at the vorticity node.

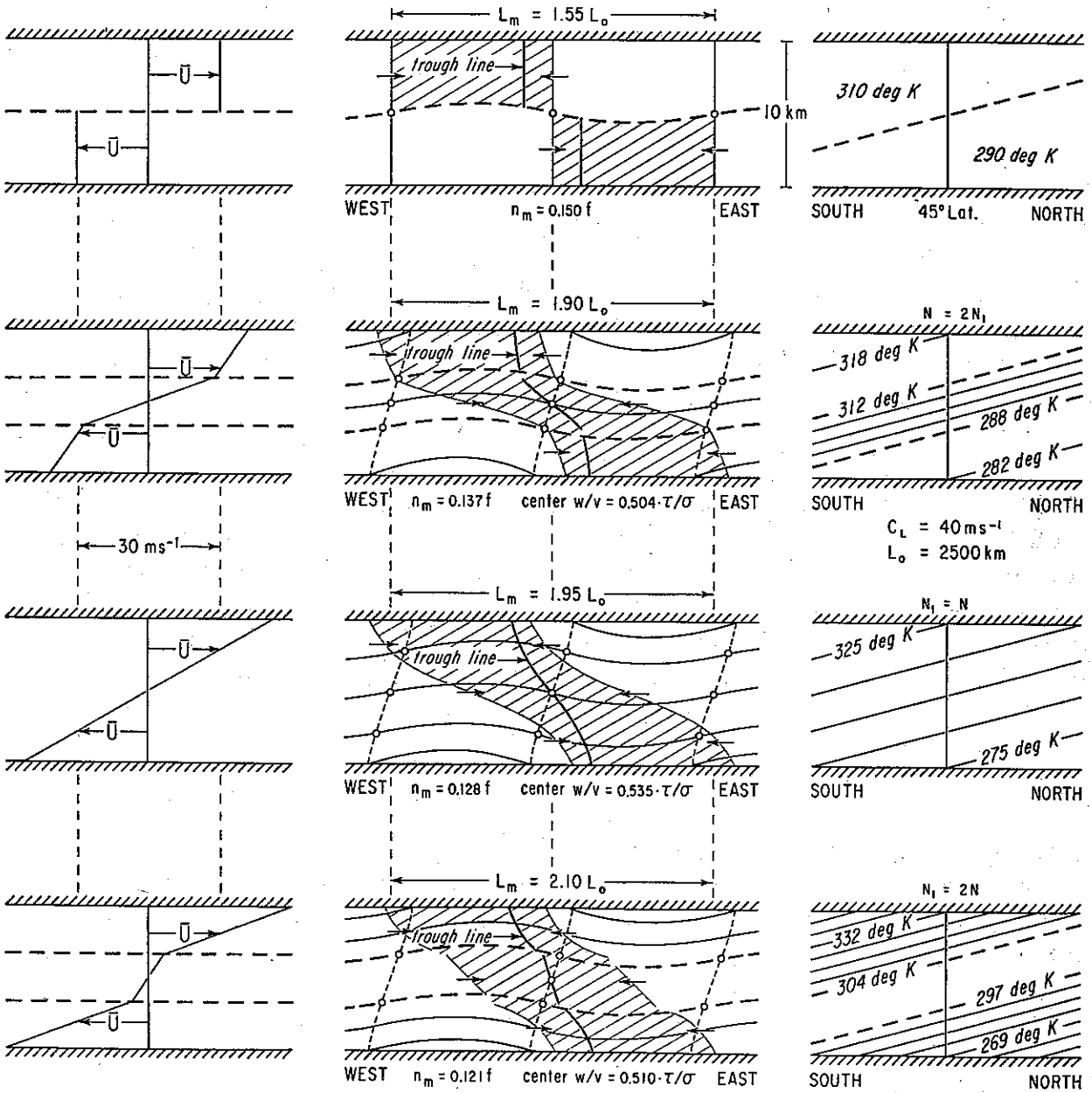


Fig. 4. The kinematic structure of the fastest growing wave in four baroclinic models with parallel isentropes.

In an arbitrary state of a symmetric wave in a model with parallel isentropes the growth and propagation of the vorticity field are known from (4.4), and the amplitude and relative phase of the divergence field is then obtained from (8.2). In particular, in the stationary state of the growing mode the relative phase of the divergence field is

$$\begin{aligned} &z<d: && \tan\phi_s=\sqrt{-ab}/\xi, \\ &z>d: && \tan\phi_s=\sqrt{-ab}/(\kappa+r\eta). \end{aligned} \tag{8.4}$$

$$n=\sqrt{-ab}\quad (kU/\kappa).$$

And the divergence-vorticity amplitude ratio in the growing mode, by elimination of $\phi$ in (8.2) is

$$\begin{aligned} &|z|<d: && D/V=(\xi^2-ab)^{\frac{1}{2}}(U/Nd). \\ &|z|>d: && D/V=[(\kappa+r\eta)^2-ab]^{\frac{1}{2}}(U/Nd). \end{aligned} \tag{8.5}$$

The kinematic structure of the fastest growing wave in four models with the same overall static stability ($C_L=40ms^{-1}$) and the same kinetic energy of zonal motion ($\bar{U}=15ms^{-1}$) is shown in Fig. 4. The upper model is the two-isentropic-layer model with the entropy change concentrated in a sharp frontal surface in the middle. The third model from the top is Eady's one-layer model. The remaining two models are three-layer models with equal depths of the layers ($\delta=2$), one with the outer buoyancy one half of the center buoyancy, and one with the outer buoyancy twice the center buoyancy. The growth rates for other wave lengths in these four models are shown in Fig. 3. All the four models have a remarkably similar structure. The wave trough tilts about a sixth of a wave length upwind (toward the west) from the lower to the upper 'equivalent' levels where $U(z)=\bar{U}$. The divergence field has a much greater upwind tilt to keep the wave stationary (see 8.4), while the temperature field tilts gently downwind in response to growing inflation of the isentropic layers in the region of convergence. The warm air to the east of the wave trough is rising and the cold air to the west of the trough is sinking, resulting in release of potential energy, which is needed to keep the wave growing.

**9. The normal modes in general symmetric three-layer models.** The evolution of symmetric waves in the center layer of these are governed by the equations (3.6), where (from 3.2) the amplitude functions $A$ and $B$ are related to the amplitude and phase of the vorticity field by

$$A\cosh\xi=V\cos\theta\,; \qquad B\sinh\xi=V\sin\theta\,. \tag{9.1}$$ (see 4.2)

In a state of stationary phase ($\theta_t=0$, $\theta=\theta_s$) the amplitude change (from 3.6) is governed by the equations

$$p\kappa V_{tt}-(aq\tanh\kappa)V=(pb'+\kappa q\tanh\kappa)V_t\cdot\coth\xi\tan\theta_s,$$

$$q\kappa V_{tt}-(bp\coth\kappa)V=-(qa'+\kappa p\coth\kappa)V_t\cdot\tanh\xi\cot\theta_s.$$

These have solutions of the form $V\sim e^{nt}$, where the growth rate $n$ is a root of the simultaneous quadratic equations

$$\begin{aligned} &p\kappa n^2-aq\tanh\kappa=n(pb'+\kappa q\tanh\kappa)\coth\xi\tan\theta_s, \\ &q\kappa n^2-bp\coth\kappa=-n(qa'+\kappa p\coth\kappa)\tanh\xi\cot\theta_s, \end{aligned} \qquad (n=n/kU) \tag{9.2}$$

or with $\theta_s$ eliminated, $n$ is a root of a bi-quadratic equation which, with the parameters $a$, $b$, etc. substituted from (3.7), takes the form

$$n^4\kappa^2+n^2[\kappa^2+a'b'-(\rho-1)(\gamma-\kappa)(p^{-1}+q^{-1})]+ab=0. \tag{9.3}$$

In the special models with parallel isentropes, $R=r^2$, $\rho=1$, $a'=a$, $b'=b$ this bi-quadratic equation becomes

$$(n^2+1)(\kappa^2n^2+ab)=0. \qquad (Uk=1)$$

The second factor gives the growth rate of the normal modes in (6.3).

In the more general $(R\neq r^2)$-models the stability boundary wave is given by the equation $a=0$, and the longer $(a<0)$ waves are unstable.

For the very long waves we introduce the abbreviations

$$\varepsilon\equiv\frac{1}{3}\kappa^2R(R-r^2)\delta^3\,; \qquad 0(\kappa^4)\equiv\text{order of }\kappa^4. \tag{9.4}$$

The parameters in (3.7) and (9.3) for the very long waves have the values

$$a=-1+\kappa^2(1+2\delta+R\delta^2)+\varepsilon+0(\kappa^4), \qquad a'=a-\varepsilon+0(\kappa^4),$$

$$\kappa\to0: \qquad b=(\kappa\bar{U}/U)^2+0(\kappa^4), \qquad b'=b-\varepsilon(1+\delta)^{-1}+0(\kappa^4), \qquad \text{(see 1.5)} \tag{9.5}$$

$$a'b'=ab+\varepsilon(1+\delta)^{-1}+0(\kappa^4), \qquad (\rho-1)(\gamma-\kappa)(p^{-1}+q^{-1})=\varepsilon(1+\delta)^{-1}+0(\kappa^4).$$

With these substituted, (9.3) becomes

$$\kappa\to0: \qquad \kappa^2n^4+n^2[\kappa^2+ab+0(\kappa^4)]+ab=0, \qquad (n=n/kU)$$

which, to the order of $\kappa^2$ has the solution

$$\kappa\to0: \qquad (\kappa n/kU)^2=-ab=(\kappa\bar{U}/U)^2. \tag{9.6}$$

Thus, in all three-layer models the longest waves have the limiting growth rate $n=k\bar{U}$, independent of the buoyancy and the details of the thermal wind distribution in the layers.

The physical reason for this simple behavior of the very long waves may be seen from the kinematic structure of these waves. From the upper equation in (9.2) the stationary phase $\theta_s$ of the center layer vorticity field in the normal mode is given by

$$\tan\theta_s=-\frac{a}{\kappa n}\cdot\frac{\kappa q\tanh\kappa-p(n\kappa)^2/a}{\kappa q\tanh\kappa+pb'}\cdot\tanh\xi. \qquad (n=n/kU) \tag{9.7}$$

For the very long modes, using the approximations in (9.5,6), we have $n\kappa=\sqrt{-ab}$ and $pb'=pb+0(\kappa^3)$ so, with higher powers of $\kappa$ ignored, the vorticity phase of the very long modes is given by

$$\kappa\to0: \qquad \tan\theta_s=\sqrt{-a/b}\tanh\xi=Uz/\bar{U}d.$$

To the same approximation the center layer vorticity field, as in (7.3), is

$$\kappa\to 0,\ |z|<d: \qquad v=V_0 e^{nt}\sec\theta_s\sin(kx+\theta_s). \qquad \tan\theta_s=Uz/\bar{U}d.$$

The isentropic contours (from 2.4) have the meridional slope

$$\kappa\to 0,\ |z|<d: \qquad Y_x=(d/U)v_z=(V_0/\bar{U})e^{nt}\cos kx=A_c k\cos kx.$$

To this approximation the temperature field has no zonal tilt and its amplitude is independent of height. The contour-streamline amplitude ratio in the long modes is $A_c=A_s\sin\theta_s$, so to this approximation the streamlines are parallel to the contours at the contour nodes at all levels, and the isentropes are advected horizontally by the meridional component of the wind. This explains why the stratification (the buoyancy) has no influence on the growth and evolution of the wave.

The upwind phase of the center layer wave trough from the divergence node in the long growing mode (from 8.2) is given by

$$\cot\phi_s=(Uk/n)(z/d)=Uz/\bar{U}d=\tan\theta_s, \qquad \theta_s+\phi_s=90^0.$$

The divergence field has precisely twice the upwind tilt of the vorticity field. The divergence-vorticity amplitude ratio in the long modes (from 8.5) is

$$\kappa\to 0,\ |z|<d: \qquad D/V=k\sqrt{\bar{U}^2+U^2(z)}\,/f$$

with the center level value $(D/V)_0=k\bar{U}/f=n/f$. Since higher powers of $\kappa$ have been ignored it follows that the kinetic energy associated with the divergence field is negligible compared to the kinetic energy of the vorticity field in the very long waves.

It is shown in Appendix B that these simple rules for the very long modes in a three-layer model of the atmosphere hold for any baroclinic layer which is bounded by rigid horizontal planes and has an arbitrary distribution of buoyancy and thermal wind shear along the vertical.

The spectral boundary between the short stable and the long unstable modes (from 9.3) is given by $a=0$, or (from 3.7) more explicitly

$$(9.8)\ n=0: \qquad Kp=\rho P+(1-\rho)\gamma/\kappa. \qquad \text{Stability boundary.}$$

This equation gives the non-dimensional wave number $\kappa_s$ of the stability boundary mode as a function of the three non-dimensional ratios $\delta$, $R$, $r$ in (1.1) for the model. The wave number $\kappa_0$ of the gravity wave with the frequency $f$ for the same model is obtained from (A.2). The corresponding wave length $L_s$ in units of the wave length of the gravity wave with the frequency $f$ is shown by the dash-dot line in Fig. 5 as a function of the buoyancy ratio $r=N_1/N$ in models with the *same thermal wind* in the layers ($R=1$), and with equal depths of the three layers ($\delta=2$). We note that here the stability boundary moves toward shorter waves and the model becomes more unstable as the buoyancy is concentrated in the outer layers, while the overall static stability, measured by the speed of the gravity waves, remains the same. The same tendency is reflected by the values of the growth rate, as computed from (9.3), for five

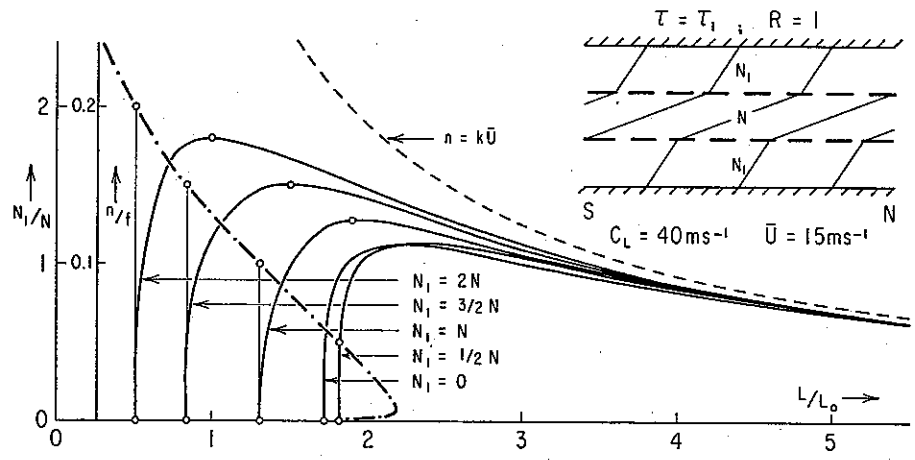


Fig. 5. Stability boundary and growth rate in models with the same thermal wind in the layers, and equal depths of the layers.

of these models with the buoyancy ratios $r=2$, 1.5, 1, 0.5, 0, all having the same static stability ($C_L=40ms^{-1}$), and the same mean zonal kinetic energy ($\bar{U}=15ms^{-1}$). All the five growth rate curves for these models approach the limiting asymptotic ($n=k\bar{U}$)-hyperbola, but the growth rate of the fastest growing mode is strongly effected by the buoyancy ratio of the layers, in particular when the outer layers have the greater buoyancy ($r>1$). This effect was also noted by EADY (l.c.), who examined a three-layer model with unbounded outer layers and the same thermal wind in the layers. Eady's unbounded three-layer model is stable for all wave lengths if the center layer has the greater buoyancy. Eady concluded that a necessary condition for baroclinic instability is minimum buoyancy in the center region. However, as we have seen, in bounded systems this is no longer true.

**10. The kinematic structure of the growing modes in general symmetric three-layer models.** The center layer meridional velocity (the vorticity field) in the growing mode (from 3.2) is

$$(10.1)\quad |z|<d: \qquad v=V_0e^{nt}\cosh\xi\sec\theta_s\sin(kx+\theta_s), \qquad (a<0)$$

where $n$ is the positive real root of the growth rate equation in (9.3), and $\theta_s$ is the corresponding stationary phase given by (9.2), namely

$$(10.2)\quad |z|<d: \qquad \tan\theta_s=\frac{p\kappa n^2-aq\tanh\kappa}{n(pb'+\kappa q\tanh\kappa)}\cdot\tanh\xi=\frac{B}{A}\cdot\tanh\xi \qquad (kU=1).$$

The upper layer field in (3.2) with the amplitudes $A_1$ and $B_1$ expressed in terms of the center layer amplitudes $A$ and $B$ with the aid of the boundary conditions in (3.4,5) may be written

$$(\kappa-\gamma)v=A[\kappa(\cosh\kappa\cosh\eta+r\sinh\kappa\sinh\eta)-(K+\rho r\tanh\zeta)\operatorname{sech}\alpha\cosh\kappa\cosh\zeta$$

$$+r(\rho-1)\cosh\kappa\sinh\eta+r(\kappa B_t/A)q\sinh\kappa\sinh\eta]\sin kx+$$

(10.3) $z>d$:

$$+B[\kappa(\sinh\kappa\cosh\eta+r\cosh\kappa\sinh\eta)-(K+\rho r\tanh\zeta)\operatorname{sech}\alpha\sinh\kappa\cosh\zeta+$$

$$+r(\rho-1)\sinh\kappa\sinh\eta-r(\kappa A_t/B)p\cosh\kappa\sinh\eta]\cos kx\,.$$

It is a smooth continuation of the center layer field at the upper boundary of the center layer $z=d$, where $\eta=0$ and $\zeta=-\alpha$. In the case of models with parallel isentropes, with the values of $A_t$ and $B_t$ substituted from (3.9), the field in (10.3) simplifies to the upper layer field in (7.5). In the growing mode $A$ in (10.3) has the value $V_0e^{nt}$ in (10.1) and the amplitude ratio $B/A$ has the value in (10.2). With these values substituted, (10.3) determines the amplitude and phase of the vorticity field at every level of the upper layer. With the vorticity field known the isentrope contour field is obtained from the thermal wind formula in (2.4), precisely as in section 7. Finally the divergence field in the growing mode is obtained from (8.2).

Two examples of the kinematic structure of the fastest growing mode in models with the same thermal wind shear in the layers and with equal depths of the layers are shown in Fig. 6. In the upper model the outer buoyancy is one half of the center buoyancy. In the lower model the outer buoyancy is twice the center buoyancy. The corresponding models with the same buoyancy ratios and with parallel isentropes, shown in Fig. 4, have been repeated in Fig. 6. All the four models have the same overall static stability ($C_L=40ms^{-1}$) and the same kinetic energy of the zonal thermal wind ($\bar{U}=15ms^{-1}$). The wave structure and growth mechanism are fairly similar in the four models in Fig. 6. However, while the instability of a model with parallel isentropes is only moderately affected by radical variations of the vertical distribution of the entropy gradient, similar variations in models with a constant thermal wind shear produce much stronger modifications in the opposite sense. The reason for this difference is discussed in the following section.

**11. The conversion from potential energy to kinetic energy in the growing unstable modes.** The kinematic structure of the growing mode is such (see Figs. 4 and 6) that warm air rises east of the wave trough and cold air sinks west of it, resulting in release of potential energy, which is needed to keep the wave growing. To examine this mechanism of potential energy release quantitatively we shall use a simple model of air parcel interchange, which was suggested by GREEN [3]: If any two air parcels in the undisturbed field in section 1 could be interchanged adiabatically without disturbing the pressure field, their mass ratio would be the inverse of the ratio of their potential temperatures,

$$M_2/M_1=\theta_1/\theta_2\,.$$

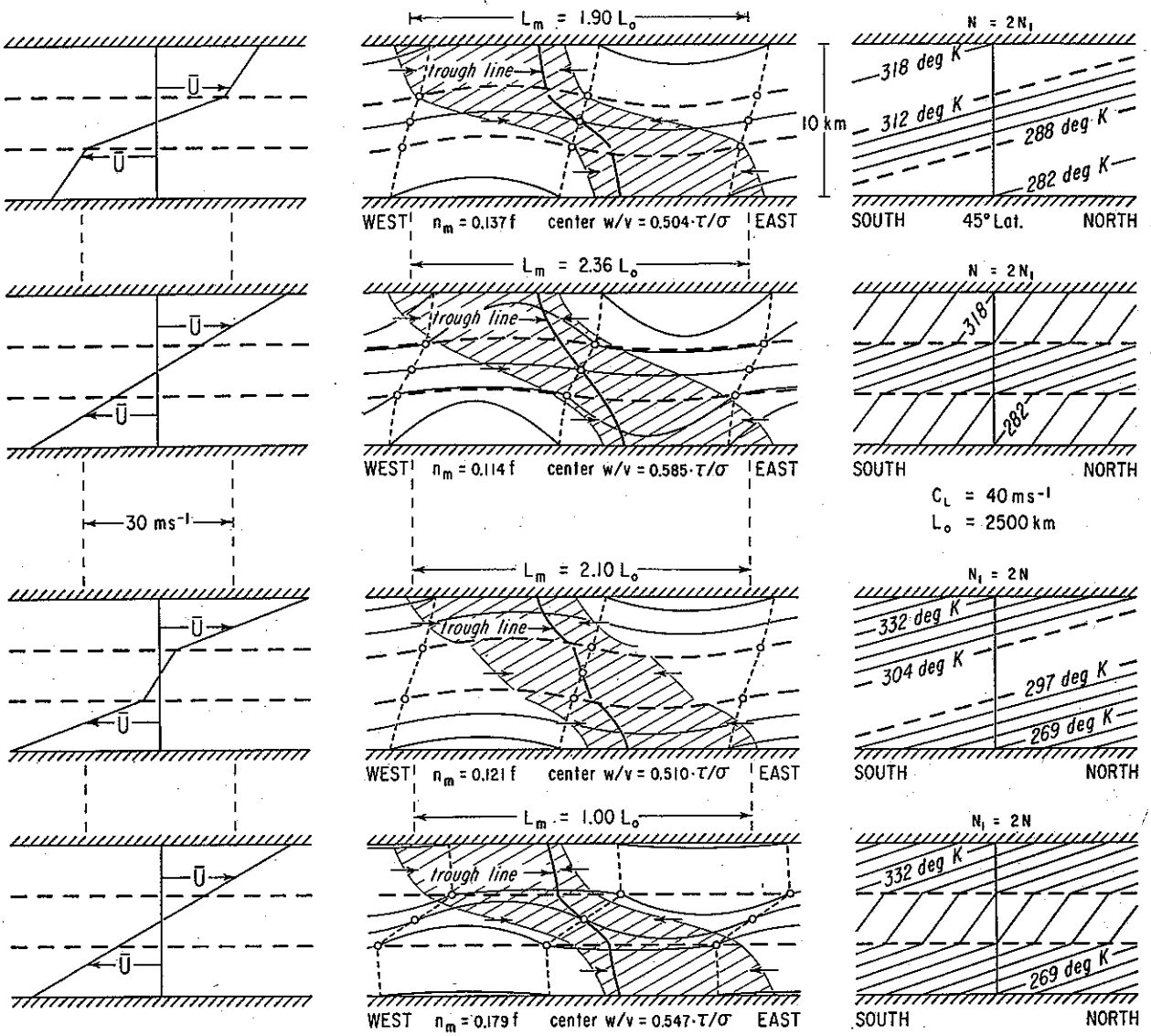


Fig. 6. The kinematic structure of the fastest growing wave in two models with the same thermal wind in the layers. The corresponding two models with parallel isentropes have been repeated from Fig. 4.

If the masses are very small, and their linear distance $s$ is small, the release of potential energy from the interchange of the parcels would be

$$-\Delta P = gs \sin\beta(M_2 - M_1) = M(N_s)^2 \sin\beta(\tan\alpha\cos\beta - \sin\beta),$$

where $\alpha$ is the isentropic slope and $\beta$ is the parcel interchange 'streamline' slope. The release of potential energy is maximum when $\beta = \frac{1}{2}\alpha$, namely

$$-\Delta P_{max} = \tfrac{1}{2}M(Ns)^2(\sec\alpha - 1) = M(\tfrac{1}{2}sN\tan\alpha)^2 + 0(\alpha^4).$$

If this released potential energy were converted into kinetic energy of the two air parcels in such a way that their speed would grow exponentially at the rate $n$, that is $v_t = nv = ns_t$, or $v = ns$, their total gain of kinetic energy after the interchange would be

$$\Delta K = 2M(\tfrac{1}{2}v^2) = M(sn)^2 = -\Delta P_{max}.$$

The corresponding local growth rate would have the value

(11.1) Parcel interchange: $n = \frac{1}{2}N\tan\alpha = \frac{1}{2}fU_z/N$. $(\tan\alpha = \tau/\sigma)$

In the three-layer models with parallel isentropes the unstable modes have the growth rates in (6.3), which may be written

(11.2) Growing mode ($R=r^2$): $n = \sqrt{-ab}\cdot N\tan\alpha$.

The meridional streamline slope in the growing mode (from 2.4) is $w/v = (1-nY/v)\tan\alpha$ which, in models with parallel isentropes, (from 7.3) has the center layer value

(11.3) $R=r^2$, $z=0$: $w/v = (1+a)\tan\alpha$. $(\tan\alpha = \tau/\sigma)$

For the fastest growing mode in the four models with layers of equal depths which are shown in Fig. 4 the factors $\sqrt{-ab}$ and $1+a$ in these formulas have the values

| $\delta=2$, $r=\sqrt{R}$: | 0 | 0.5 | 1 | 2 |
|---|---|---|---|---|
| $(\sqrt{-ab})_{max}$: | 0.22 | 0.24 | 0.31 | 0.51 |
| $1+a$: | 0.518 | 0.504 | 0.533 | 0.510 |

In all these models the center level streamline slope in the fastest growing mode is just a little over one half of the isentropic slope. Since the streamline slope decreases uniformly from the maximum value in the middle toward zero at the rigid boundaries, it is nearly one half of the isentropic slope over a good part of the central region in the fastest growing mode. This is evidently the most efficient way the potential energy can be released by a normal mode disturbance. In the one-layer Eady model ($r=1$) the efficiency for the fastest growing mode is about 62 per cent of the maximum local value from parcel interchange.

The form of the local parcel interchange growth rate formula in (11.1) explains in a qualitative way why a model with parallel isentropes ($\alpha=$const) becomes more unstable when the buoyancy is increased in the center layer, whereas a model with the same thermal wind in the layers ($U_z=$const) becomes more stable when the buoyancy is increased in the center layer.

## APPENDIX A

### The gravity wave with the frequency f in the three-layer model

Let $C_L$ denote the limiting phase velocity of the long quasi-static gravity waves in the three-layer model in section 1, and let $k_0 = f/C_L$ denote the wave number of the gravity wave with the frequency $f$. As in (3.1) we introduce for this wave the non-dimensional wave number

(A.1) $\kappa_0 = k_0 d(N/f)$.

The quasi-static equations for the vertical velocity in this gravity wave are

$z<d$: $$w=-(f/Nk_0)^2 w_{zz}=-w_{\xi_0\xi_0}=A\cos\xi_0\,, \qquad \xi_0=(\kappa_0/d)z\,.$$

$z>d$: $$w=-(f/rNk_0)^2 w_{zz}=-w_{\zeta_0\zeta_0}=B\sin\zeta_0 \qquad \zeta_0=(r\kappa_0/d)(z-h)$$

The integration constants $A$ and $B$ are determined by continuity of the vertical velocity and its derivative across the upper boundary of the center layer, which gives

(A.2) $$\tan\kappa_0=r\cot\alpha_0\,. \qquad (\alpha_0=\delta r\kappa_0)\,.$$

In the special case when the three layers have the same buoyancy ($N=N_1$) the model is a one-layer model, and the wave number of the gravity wave with the frequency $f$ is here given by

(A.3) $r=1$: $$\tan\kappa_0=\cot\delta\kappa_0\,, \qquad \text{or } \kappa_0(1+\delta)=k_0h(N/f)=\tfrac{1}{2}\pi\,.$$

With the rigid tropopause 10 km above the ground ($h=5$ km) and a potential temperature increase of about 50 deg $K$ from the ground to the tropopause the limiting phase velocity of the gravity wave in this one-layer model is about 40 $ms^{-1}$. In the more general three-layer models the limiting phase speed of the gravity wave may be regarded as a measure of the overall static stability of the model, and we may take $C_L=40\ ms^{-1}$ as a typical value which reflects observed atmospheric conditions. The corresponding length of the gravity wave with the frequency $f$ in middle latitudes is about $L_0=2500$ km.

## APPENDIX B

### The long normal modes in a baroclinic layer which is bounded by rigid horizontal planes

We use the same notations as in section 1. The layer has the depth 2h. We use a frame of reference with the origin ($z=0$) at the center level and moving with the center of gravity of the layer. Consistent with the Bousinesq approximation the mean kinetic energy of the balanced zonal motion in this frame is

(B.1) $$\bar{U}^2=\tfrac{1}{2}\int_{-1}^{+1} U^2(\xi)d\xi\,; \qquad \int_{-1}^{+1} U(\xi)d\xi=0\,. \qquad \xi=z/h\,.$$

The normal modes in this layer are small-amplitude sinusoidal wave disturbances with the time dependency $\exp(nt)$, where the growth rate $n$ may be real or complex. For the individual time derivative of the wave elements in the normal mode we introduce the abbreviation

(B.2) $$\frac{D}{Dt}(\ )=v(\ )_x\,; \qquad v=U(z)-in/k\,,$$

where $k$ is the zonal wave number. The normal modes we consider have no variation with latitude.

The adiabatic equation in (2.3), also using (2.4), may be written

$$\sigma w=\tau(v-vY_x)=\tau(v-vv_z/U_z),$$

where the entropy gradients $\tau$ and $\sigma$ are here arbitrary functions of height. Substitution from (1.2) of $g\tau=fU_z=fv_z$ gives

(B.3) $$N^2w=f(vv_z-vv_z)=-fv^2(v/v)_z. \qquad N=\sqrt{\sigma g}.$$

The vorticity equation (2.5), within the accuracy of the Bousinesq approximation, is

(B.4) $$vv_{xx}+\beta v=-k^2(v-U_R)v=fw_z. \qquad (U_R=\beta/k^2)$$

Elimination of $v$ from (B.3,4) gives the differential equation for the vertical velocity in the quasi-geostrophic normal modes, namely

(B.5) $$v^2[w_\xi(v^2-U_Rv)^{-1}]_\xi=K^2w. \qquad K=kh(N/f).$$

In the limit, for the very long modes, this equation has the integral

(B.6) $K\to 0$: $$w_\xi=\text{const.}(v^2-U_Rv)e^{ikx+nt}, \qquad (\xi=z/h)$$

and a second integral between the rigid boundaries gives the growth rate equation

(B.7) $K\to 0$: $$\int_{-1}^{+1}(v^2-U_Rv)d\xi=0.$$

If the $\beta$-effect is ignored ($U_R\to 0$) this integral, with $v$ substituted from (B.2), gives the growth rate $n=k\bar{U}$, where $\bar{U}^2$ (from B.1) is the mean kinetic energy of the zonal wind in a frame which moves with the center of gravity of the layer.

With $w_z$ substituted from (B.6), the vorticity equation (B.4) gives the meridional velocity in the very long modes. If the $\beta$-effect is ignored, the meridional velocity is the real part of

$K\to 0$, $U_R\to 0$: $$v=\text{const. }ve^{ikx+nt}=V_0e^{nt}[U(z)/\bar{U}-i]e^{ikx},$$

which may be written

$K\to 0$, $U_R\to 0$: $$v=V_0e^{nt}\sec\theta_s\sin(kx+\theta_s); \qquad \tan\theta_s=U(z)/\bar{U}.$$

From (2.4) the isentropic contours have the meridional slope

$K\to 0$, $U_R\to 0$: $$Y_x=v_z/U_z=(V_0/\bar{U})e^{nt}\cos kx=A_ck\cos kx.$$

The temperature wave has no zonal tilt, and at all levels it has the same constant amplitude $A_c=A_s\sin\theta_s$ which grows at the rate of the meridional wind at the crest ($A_{ct}=V_0e^{nt}$). Finally from (8.2,3,4), which hold for all laterally unbounded waves, the relative phase and amplitude of the divergence field in the very long modes are

$K\to 0$, $U_R\to 0$: $$\phi_s=90^0-\theta_s; \qquad D/V=k\sqrt{\bar{U}^2+U^2(z)}\,/f.$$

The divergence field has precisely twice the upwind tilt of the vorticity wave and its amplitude is negligible compared to the vorticity amplitude.

This simple theory for the long modes in arbitrary baroclinic layers is a generalization of FJØRTOFT's theory for a baroclinic layer with zero static stability [2] (the so-called advective model). The long mode growth rate equation in (B.7) is identical to Fjørtoft's equation (op. cit 31.4), which holds for all quasi-geostrophic modes in the advective model. In summary then, we have shown that the very long modes in an arbitrary baroclinic layer in the limit have an advective evolution. The temperature field is advected horizontally by the meridional component of the wind. The vertical velocity associated with the divergence field which keeps the tilting vorticity wave stationary growing at the rate $k\bar{U}$ is so weak that it gives no significant contribution to the rate of deformation of the temperature field.

When the dynamic effect of the planetary vorticity gradient is included in the theory for the long normal modes ($\beta \neq 0$), the integral in (B.7) gives for the growth rate $n$ in these modes

(B.8) $K \to 0$, $\beta \neq 0$: $$(n/k - \tfrac{1}{2}iU_R)^2 = \bar{U}^2 - \tfrac{1}{4}U_R^2. \qquad (U_R = \beta/k^2).$$

If the overall thermal wind shear $\bar{U}$ in the baroclinic layer is sufficiently great, this formula gives a fairly good approximation in the spectral region of the special wave number

(B.9) $$k_b^2 = \tfrac{1}{2}\beta/\bar{U} \ll (f/Nh)^2$$

The wave with this wave number $k_b$ in (B.9) then marks the spectral boundary between longer stable modes and shorter unstable modes. The mode on this upper boundary of the unstable spectral region is stationary in a frame which moves to the west with the speed $\bar{U}$ relative to the center of gravity of the layer, and has in this frame the wave elements

$k = k_b$: $$v = [U(z) + \bar{U}]A_c k \cos kx, \qquad Y = A_c \sin kx$$

$$u = (k/f)[U^2(z) - \bar{U}^2]A_c k \cos kx$$

The longer stable modes and the shorter unstable modes near this upper stability boundary have the same kinematic structure as in the advective model. These have been discussed by the author in some detail in an earlier paper [4].

## REFERENCES


1. EADY, E. T., 1949: Long Waves and Cyclone Waves. *Tellus* 1, No. 3, pp. 33–52.
2. FJØRTOFT, R., 1950: Application of Integral Theorems etc. *Geof. Publ.* 17, No. 6.
3. GREEN, J. S. A., 1960: A Problem in Baroclinic Stability. *Quart. J. R. Met. Soc.* Vol. 86, pp. 237–251.
4. HOLMBOE, J., 1959: On the Behavior of Baroclinic Waves. *The Rossby Memorial Volume*, The Rockefeller Institute Press, New York, pp. 333–349.
5. — 1966: The Growth of a Young Frontal Wave, *Tellus* 18, No. 4, pp. 830–837.

Avhandlinger som ønskes opptatt i «Geofysiske Publikasjoner», må fremlegges i Videnskaps-Akademiet av et sakkyndig medlem.

**Vol. XXII.**

No. 1. L. Harang and K. Malmjord: Drift measurements of the E-layer at Kjeller and Tromsø during the international geophysical year 1957—58. 1960.
» 2. Leiv Harang and Anders Omholt: Luminosity curves of high aurorae. 1960.
» 3. Arnt Eliassen and Enok Palm: On the transfer of energy in stationary mountain waves. 1961.
» 4. Yngvar Gotaas: Mother of pearl clouds over Southern Norway, February 21, 1959. 1961.
» 5. H. Økland: An experiment in numerical integration of the barotropic equation by a quasi-Lagrangian method. 1962.
» 6. L. Vegard: Auroral investigations during the winter seasons 1957/58—1959/60 and their bearing on solar terrestrial relationships. 1961.
» 7. Gunnvald Bøyum: A study of evaporation and heat exchange between the sea surface and the atmosphere. 1962.

**Vol. XXIII.**

No. 1. Bernt Mæhlum: The sporadic E auroral zone. 1962.
» 2. Bernt Mæhlum: Small scale structure and drift in the sporadic E layer as observed in the auroral zone. 1962.
» 3. L. Harang and K. Malmjord: Determination of drift movements of the ionosphere at high latitudes from radio star scintillations. 1962.
» 4. Eyvind Riis: The stability of Couette-flow in non-stratified and stratified viscous fluids. 1962.
» 5. E. Frogner: Temperature changes on a large scale in the arctic winter stratosphere and their probable effects on the tropospheric circulation. 1962.
» 6. Odd H. Sælen: Studies in the Norwegian Atlantic Current. Part II: Investigations during the years 1954—59 in an area west of Stad. 1963.

**Vol. XXIV.**

In memory of Vilhelm Bjerknes on the 100th anniversary of his birth. 1962.

**Vol. XXV.**

No. 1. Kaare Pedersen: On the quantitative precipitation forecasting with a quasi-geostrophic model. 1963.
» 2. Peter Thrane: Perturbations in a baroclinic model atmosphere. 1963.
» 3. Eigil Hesstvedt: On the water vapor content in the high atmosphere. 1964.
» 4. Torbjørn Ellingsen: On periodic motions of an ideal fluid with an elastic boundary. 1964.
» 5. Jonas Ekman Fjeldstad: Internal waves of tidal origin. 1964.
» 6. A. Eftestøl and A. Omholt: Studies on the excitation of $N_2$ and $N_2^+$ bands in aurora. 1965.

**Vol. XXVI.**

No. 1. Eigil Hesstvedt: Some characteristics of the oxygen-hydrogen atmosphere. 1965.
» 2. William Blumen: A random model of momentum flux by mountain waves. 1965.
» 3. K. M. Storetvedt: Remanent magnetization of some dolerite intrusions in the Egersund Area, Southern Norway. 1966.
» 4. Martin Mork: The generation of surface waves by wind and their propagation from a storm area. 1966.
» 5. Jack Nordo: The vertical structure of the atmosphere. 1965.
» 6. Alv Egeland and Anders Omholt: Carl Størmer's height measurements of aurora. 1966.
» 7. Gunnvald Bøyum: The energy exchange between sea and atmosphere at ocean weather stations M, I and A. 1966.
» 8. Torbjørn Ellingsen and Enok Palm: The energy transfer from submarine seismic waves to the ocean. 1966.
» 9. Torkild Carstens: Experiments with supercooling and ice formation in flowing water. 1966.
» 10. Jørgen Holmboe: On the instability of stratified shear flow. 1966.
» 11. Lawrence H. Larsen: Flow over obstacles of finite amplitude. 1966.

A.s John Griegs Boktrykkeri